ELECTROCHEMICAL BEHAVIOUR OF LEAD OXIDES IN APROTIC ORGANIC ELECTROLYTE SOLUTIONS

G. LUDWIG, W. SCHNEIDER and K. WIESENER*

Dresden University of Technology, Department of Chemistry, 8027 Dresden, Mommsenstrasse 13, (G.D.R.)

(Received August 1, 1986; in revised form January 20, 1987)

Summary

Of the various lead oxides tested, red lead (Pb_3O_4) proved to be the most suitable for use as cathode material in lithium cells having a voltage of 1.5 V. Based on electrochemical, chemical, and physical measurements, the reaction mechanisms of red lead cathodes are discussed. The reduction of red lead to lead is assumed to proceed in two partial steps which run simultaneously during the discharge process. While at the beginning of the discharge the reduction of Pb^{4+} to Pb^{2+} dominates, it is the reduction of Pb^{2+} to Pb in the phase interface which determines the potential in the discharge plateau. Simultaneously, Pb^{4+} is reduced in the bulk of the red lead particles.

Introduction

The use of lead oxides as positive active materials in electrochemical power sources with aqueous electrolyte solutions is important in lead accumulators. Owing to their comparatively high charge density and their high positive potential, however, they are also of interest as cathode materials in lithium cells with aprotic organic electrolytes. There is only limited knowledge of the electrochemical discharge properties of the individual lead oxides in relevant electrolyte solutions [1 - 3]. Our object was to investigate the applicability of lead oxides to lithium cells and to obtain relevant information on the discharge mechanisms.

Experimental

The Pb_2O_3 and some of the Pb_3O_4 samples used were synthesized in the laboratory by thermal decomposition of PbO_2 (4 h at 410 °C and 4 h at 490 °C, respectively). These lead oxides were chemically analysed and

---

*Author to whom correspondence should be addressed.

evaluated by means of X-ray diffraction patterns. For some of the tests industrial lead oxides (VEB Laborchemie Apolda) were also used. For the electrochemical tests the active material was mixed with carbon black (as a conductive additive) and a Teflon binder. The mixture was then pressed at 100 MPa to form cathode tablets and placed into test cells such as that shown in Fig. 1. Lithium (99.9%), contaminated by 0.01% K, 0.02% Na, 0.008% Mg, 0.01% Ca and 0.01% Fe was used as the anode material. Lithium was provided in excess to prevent limitation of the cell capacity.
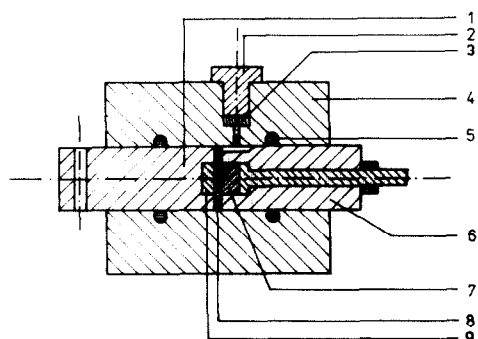

Fig. 1. Test cell — sectional view. 1, V2A cathode cup; 2, sealing screw; 3, lithium stopper; 4, polyethylene hollow cylinder; 5, sealing ring; 6, polyethylene cylinder with V2A collector; 7, lithium anode; 8, separator with electrolyte; 9, cathode.

1 M solutions of $LiClO_4$ in a mixture of polypropylene carbonate (PC) and dimethoxyethane (DME) (37:63 or 50:50 per cent. by volume) were used as electrolytes (average quantity of electrolyte in the cell 600 mg) with a separator of non-woven (FS 2108) polypropylene.

The cathode mixture consisted of 92 wt.% of active material (AM), 5 wt.% of acetylene black P 1042 (VEB Stickstoffwerk, Piesteritz), and 3 wt.% of polytetrafluoroethylene from a PTFE suspension (ICI, Great Britain). The cathodes were 11 mm in diameter and 2 mm thick. Before the electrochemical test the cathode, together with the cathode cup, was dried under vacuum at 110 °C for 15 h. The anodes were prepared and the test cells assembled exclusively in an argon dry box at <100 ppm humidity as were the post-test chemical analyses. The electrochemical data were obtained by the rheostatic discharge and the galvanostatic interruption methods.

The chemical changes in the lead oxides as a function of efficiency were determined by X-ray diffraction patterns and by chemical analysis of the discharge products. Chemical determination of the metallic lead content of the discharge products was carried out after dissolution of the lead oxides in hydroxylaminehydrochloride. To dissolve the elemental lead, the filtration residue was treated repeatedly with water of low alkalinity and subsequently with hydrogen peroxide. The lead, converted in this way into Pb^{2+}, was titrated at pH 5 - 6 with komplexon II against xylenol orange.

Results and discussion

The electrochemical discharge curves of the lead oxide cathodes are shown in Fig. 2. The equation

$$PbO_x + 2xLi^+ + 2xe^- \longrightarrow Pb + xLi_2O \qquad (1)$$
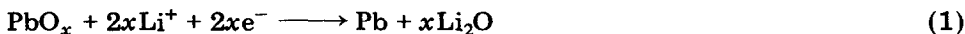
was used to calculate the efficiency of the lead oxide. Considering its high specific charge and high specific energy, PbO_2 should possess the most favourable properties for use as a cathode material.

With all used lead oxide materials a discharge plateau is observed at 1.5 V. In accordance with other authors [1 - 3], who used different electrolyte solutions, efficiencies of greater than 80 per cent. were obtained up to the final discharge voltage of 1.0 V. Cathodes with PbO (red), Pb_2O_3, or Pb_3O_4 as active materials gave a very high efficiency, sometimes more than 100%. This appeared to be caused by the cathodic reduction of polypropylene carbonate [4, 5] and/or by the electrochemical formation of lead–lithium compounds [6].

With all lead oxide materials, a drop in cell voltage is observed at the beginning of the discharge. α- and β-PbO_2 show an initial discharge plateau near 2.5 V which should be formed more distinctly in the case of PbO_2 due to the high Pb^{4+} concentration. This highlights the reaction of PbO_2 with the lead at the phase interface according to the equation

$$PbO_2 + Pb \longrightarrow 2PbO \qquad (2)$$

With the other lead oxides the discharge plateau, near 1.5 V, is reached more rapidly as the average oxidation number of lead in PbO_x is lowered. Longer
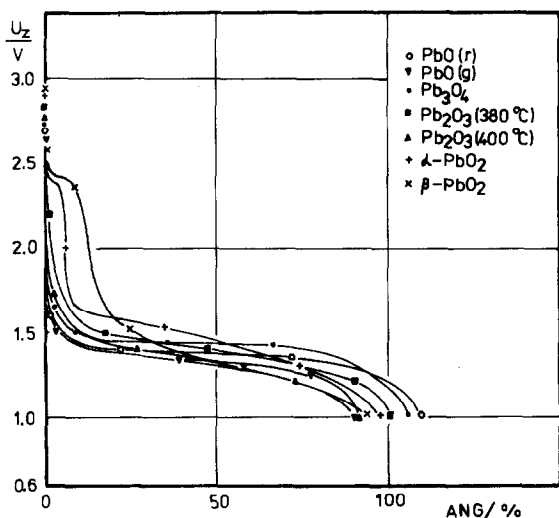

Fig. 2. Cell voltage, U_z, as a function of efficiency (ANG) in test cells with lead oxide cathodes (92 wt.% of active material (lead oxides), 5 wt.% of acetylene black P 1042, 3 wt.% of PTFE). p = 100 MPa; R = 5.6 kΩ; electrolyte: 1 M $LiClO_4$–PC/DME (50:50).

horizontal discharge plateaux were also found with the lead oxides of lower valence.

The chemical and X-ray-diffraction analyses of the discharge products confirmed the formation of elemental lead. Owing to the high specific charge at a definate cell voltage plateau of 1.5 V, red lead (Pb_3O_4) was selected for further electrochemical tests. The galvanostatic interruption method [7], which allows the reactions and changes in cathode structure during the discharge process to be assessed, was applied. Information can be obtained from the change in potential (ΔU) during an interruption time (t_0). The discharge potential, U_{Li} (lithium reference electrode), and the potential difference, ΔU, (1000 μs after opening of the circuit), are plotted as a function of the efficiency for red lead at two current densities in Fig. 3. The ΔU/efficiency curves clearly show the decrease in potential difference, ΔU, after the beginning of the discharge process. At a discharge time of $t_{e1}{}^{min}$ a further drop in ΔU is observed, but after ΔU reached a minimum at $t_{e2}{}^{min}$ it increased to a maximum at $t_e{}^{max}$ then decreased.
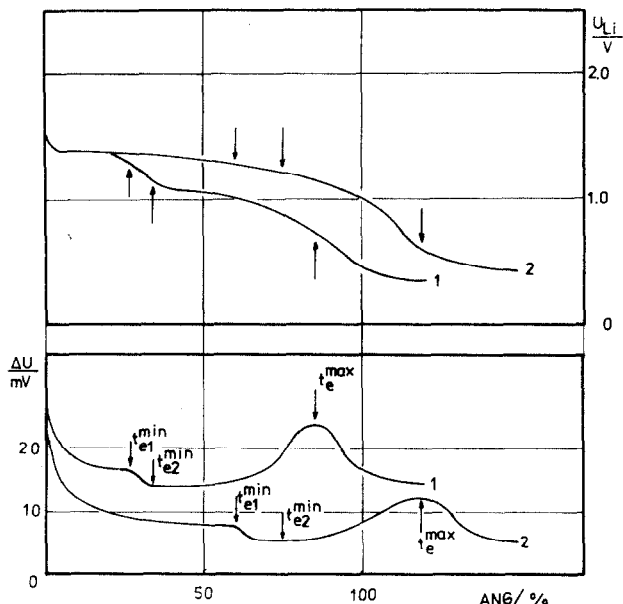

Fig. 3. Discharge potential U_{Li} (lithium reference electrode) and potential difference ΔU (between 0 and 1000 μs after interruption) of red lead cathodes (92 wt.% red lead; 5 wt.% acetylene black P 1042; 3 wt.% PTFE) as a function of efficiency (ANG) at discharge current densities of 1 mA cm^{-2} (1) and 0.2 mA cm^{-2} (2). Electrolyte: 1 M LiClO$_4$–PC/DME (37:63).

The discharge times $t_{e1}{}^{min}$, $t_{e2}{}^{min}$ and $t_e{}^{max}$ are characterized by the potential values of the working electrode of about 1.25 V, 1.15 V and 0.85 V, respectively.

Figure 4 shows the potential difference of the working electrode (i = 1 mA cm^{-2}) during interruption of current (t_0 = 1000 μs) as a function of

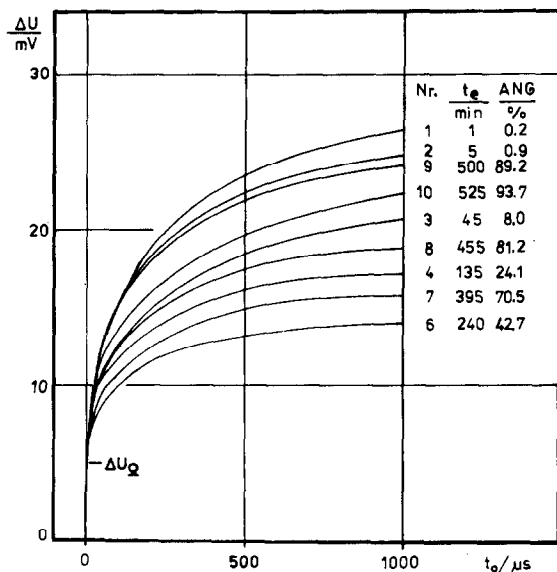| Nr.	t_e	ANG
	min	%
1	1	0.2
2	5	0.9
9	500	89.2
10	525	93.7
3	45	8.0
8	455	81.2
4	135	24.1
7	395	70.5
6	240	42.7

Fig. 4. Change of the potential difference, ΔU, of the red lead cathode (Fig. 3; $i = 1$ mA cm^{-2}) during interruption ($t_0 = 1000$ μs) as a function of discharge time t_e and efficiency (ANG) ΔU_Ω: ohmic voltage drop.

efficiency and discharge time. It can be seen that the ohmic voltage drop $\Delta U = IR_i$, which occurs 10^{-8} s after current interruption, is a constant 5 mV during the discharge time. We conclude that the electronic conductivity of the cathode is determined mainly by that of the acetylene black, P 1042. The change of the potential difference during the discharge process is therefore based on the electrode kinetics only. In principle, changes in the chemical composition during discharge are determined according to the cathodic reaction equation

$$Pb_3O_4 + 8Li^+ + 8e^- \longrightarrow 3Pb + 4Li_2O \tag{3}$$

The changing chemical composition on the one hand causes the variation of the ohmic resistance and dielectric constant and, on the other hand, indirectly influences the transport processes, *i.e.*, the electrolyte transport (influence of the secondary structure of the electrode) and the migration of the lithium ions in the solid (influence of the primary structure of the electrode).

Both the X-ray diffraction patterns (Fig. 5) and the chemical analysis (Fig. 6) show lead to be a reaction product. Figure 5 shows that with increasing efficiency (ANG) the reduction product (Pb) peak (18.3°) increases, and that of the reactant (Pb_3O_4) (15.4°) decreases. The peak at 16.8°, belonging to both PbO and to Pb_3O_4, decreases more slowly than the peak at 15.4° (Pb_3O_4 only). This implies that in the first reduction step PbO occurs as a reaction product. In Fig. 6 it can be seen that the Pb^{2+} content is constant at the beginning of discharge up to an efficiency (ANG) of about 50%.
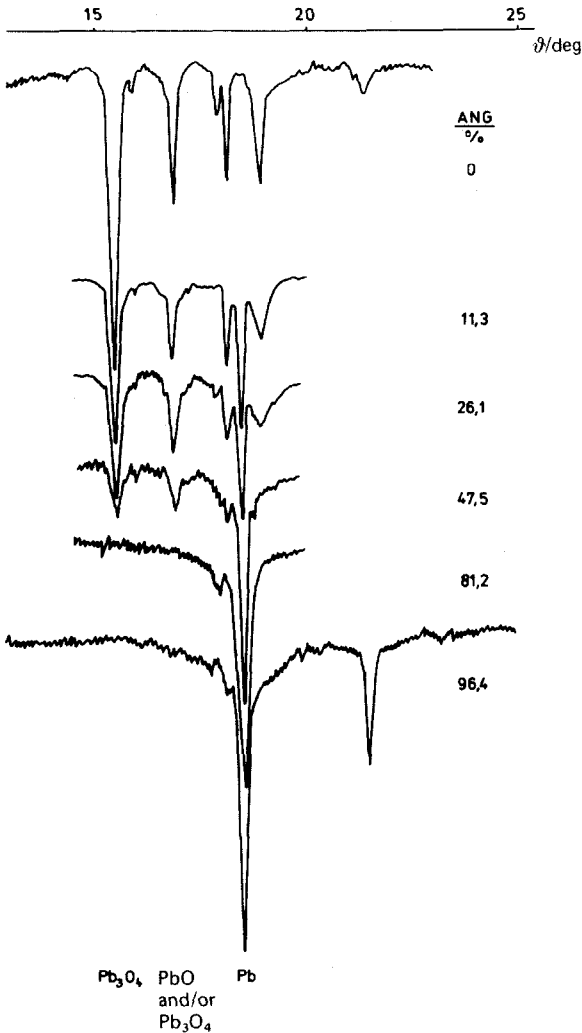
Fig. 5. X-ray diffraction patterns of red lead cathodes (92 wt.% red lead; 5 wt.% acetylene black P 1042; 3 wt.% PTFE) as a function of efficiency (ANG).

As lead has a higher density than red lead, an increase in cathode porosity is to be expected with increased discharge time, *i.e.*, owing to discharge the reaction surface is renewed by the cracking of the lead layer on the particle surface. This would also explain the comparatively high efficiency of the red lead cathodes. Simultaneously, the conductivity of the cathode should rise and the IR-value should decrease, since lead is a very good electronic conductor. As can be seen from Fig. 4, however, the IR-drop remains constant during the interruption time t_0 as a function of the discharge time, t_e.

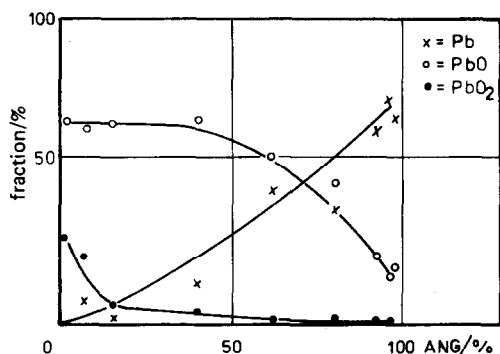From the results we conclude that the variation in potential difference, ΔU, is caused by four factors:

Fig. 6. Pb-, PbO-, and PbO_2-fractions in red lead as a function of efficiency.

(i) An accelerated charge transfer reaction dominates up to the discharge time $t_{e_1}^{min}$. The potential difference, ΔU, decreases due to changes in the stoichiometry of the lead oxide and to the decrease in polarization resistance. This is supported by the decrease of the time constants of the current–interruption curves (Fig. 4) being accompanied by the swelling of the cathode during discharge, a phenomenon which is always observed. This results in a better electrolyte diffusion into the cathode material.

(ii) An improved specific conductivity of the cathode due to the formed reaction product of lead. This becomes evident by the fact that ΔU drops once more to the discharge time $t_{e_2}^{min}$. The detection of the resulting reduction of the IR drop is difficult since the changes of ΔU are low due to the limited resolution of the oscilloscope.

(iii) That ΔU rises again up to t_e^{max} is attributed to the continuous reduction of the reaction area due to the formation of the reaction product of lead, observable by the increase of the local current density of the charge transfer. The metallic lead formed on the surface is a non-ion-conducting top layer which is electron conducting down to a cell voltage of 0.8 V, but which blocks electrochemical processes. With increasing discharge time the effect of surface reduction increases and results in a high ΔU rise due to the increase of overvoltage of the charge transfer. An increase of the polarization resistance (Fig. 4) connected with the surface reduction at constant current discharge is likely to increase this effect.

(iv) At discharge time t_e^{max} the major part of the reaction area is covered with lead. Due to the progressing conversion of the oxide, the discharge potential drops so much that intercalation of lithium into the lead lattice becomes possible as a new reaction. As the whole reaction surface of lead is available for the reaction according to eqn. (4) [6, 8] there is again a decrease in potential difference ΔU.

$$Pb + x Li^+ + x e^- \longrightarrow Li_x Pb \tag{4}$$

The discharge mechanism of red lead in aprotic organic lithium salt solution can be explained by the model below:

The reduction of red lead begins at the phase interface of the electrolyte/red lead particles. At first Pb^{4+} is reduced to Pb^{2+} under the simultaneous formation of Li_2O. This reduces the Pb^{4+} concentration in the phase interface, and the dominating Pb^{2+} (Figs. 5 and 6) determines the potential of the electrode. This is associated with a drop in the electrode potential to 1.5 V (against lithium) reflected in the discharge characteristics (Fig. 3). Further discharge continues to reduce the red lead towards the interior of the particles by charge transport. Since, therefore, only Pb^{2+} ions can be electrochemically reduced in the phase boundary, the discharge potential of the Pb^{2+}/Pb reduction remains constant until all the Pb^{2+} ions are used up. Only when the red lead is almost completely discharged is the potential decreased, and a lead–lithium alloy formed.

References

1 T. Ohzuku, T. Shimamoto and T. Hirai, *Electrochim. Acta, 26* (1981) 751.
2 M. Broussely, Y. Jumel and J. P. Gabano, *Power Sources 7*, Academic Press, London, 1979, p. 637.
3 L. P. Bicelli, B. Rivolta, F. Bonino, S. Maffi and C. Malitesta, *J. Power Sources, 18* (1980) 63.
4 G. Eichinger, *J. Electroanal. Chem., 74* (1976) 183.
5 A. N. Dey and P. B. Sullivan, *J. Electrochem. Soc., 117* (1970) 222.
6 A. N. Dey, *J. Electrochem. Soc., 118* (1971) 1547.
7 J. Garche, G. Schädlich, K. Wiesener, H. Kaden and W. Oelsner, *J. Electroanal. Chem., 180* (1984) 587.
8 J. G. Kiseleva, N. N. Tomaseva and B. N. Kabanov, *Elektrokhimiya, 19* (1983) 532.